August 31, 2012

HICO User Annual Report

Using HICO data for the preparation of the future EnMAP satellite mission

Nicole Pinnel[1], Rolf Richter[1], Slava Kiselev[2], Martin Bachmann[1]

[1]DLR, Earth Observation Center, German Remote Sensing data Center, Oberpfaffenhofen, 82234 Wessling, Germany

[2] Earth Observation and Mapping, EOMAP GmbH, Sonderflughafen Oberpfaffenhofen, 82205 Gilching, Germany

1. Abstract

This report shows first results of pre-processing products using HICO data from Venice (AAOT) in Italy in combination with data from Aqua Alta Oceanographic Towers (AERONET-OC). The primary output of this report is a first evaluation of HICO data quality in comparison to different processing algorithms, focusing primarily on atmospheric correction methods (Tafkaa 6s, ATCOR, MIP). ATCOR atmospheric correction software was first compared to Tafkaa 6s processing on water and on land using similar input parameters. Secondly ATCOR was compared to subsurface reflectance of water processed by Modular Inversion Program (MIP).

2. Objective

The main objective of this study is to test and to evaluate the EnMAP (Environmental Mapping and Analysis Program) pre-processing chain using HICO hyperspectral data. A clear advantage in using HICO for testing the processing chain is the unique opportunity to have real hyperspectral satellite data with specifications comparable to the EnMAP VNIR sensor requirements. One of the foreseen standard products of the EnMAP processing chain is atmospheric correction on water and on land (Rossner et al. 2009; Storch at al. 2009). Three atmospheric correction methods were employed in this investigation (Tafkaa 6s, ATCOR, MIP) and applied to two different HICO scenes for comparison on land and on water. A brief overview of the three different correction methods is given below:

2.1 Tafkaa atmospheric software

Tafkaa is an atmospheric correction algorithm for remote sensing of ocean color that has been developed at the Naval Research Laboratory (NRL), particularly it is an algorithm for atmospheric correction of imaging spectrometry data. Tafkaa 6s is based on ATmospheric REMoval (ATREM) 4.0, and uses Second Simulation of the Satellite Signal in the Solar Spectrum (6S) for its scattering calculations. It cannot correct for the specular reflection of the air-water interface (Montes et al. 2004).

2.2 ATCOR atmospheric software

ATCOR (atmospheric correction) (Richter 1996; 1998, 2008, 2011) accounts for flat and rugged terrain, and includes haze/cirrus detection and removal algorithms. Output products are the ground reflectance cube, maps of the aerosol optical thickness at 550 nm, atmospheric water vapor, and masks of land, water, haze, cloud, and snow. The reflectance retrieval for land and water pixels is performed with the assumption of a Lambertian reflectance law. Contrary to the MIP processing, the water reflectance is the above surface reflectance. The atmospheric correction on land within the EnMAP pre-processing chain will be performed with the ATCOR atmospheric correction code.

2.3 Modular Inversion Program (MIP)

The Modular Inversion Program (MIP**)** (Heege et al. 2005) combines the finite element method with the MODTRAN4 atmospheric model and the multi-component water model. Output products are the water reflectance cube, water constituents, the aerosol optical thickness map, and updates of masks of land, water, haze and cloud. The MIP processing corrects the water to sub-surface reflectance. MIP will be used within the EnMAP pre-processing chain for atmospheric correction over water targets.

3. Intercomparison of calibrated radiance data (Version 03 and 04)

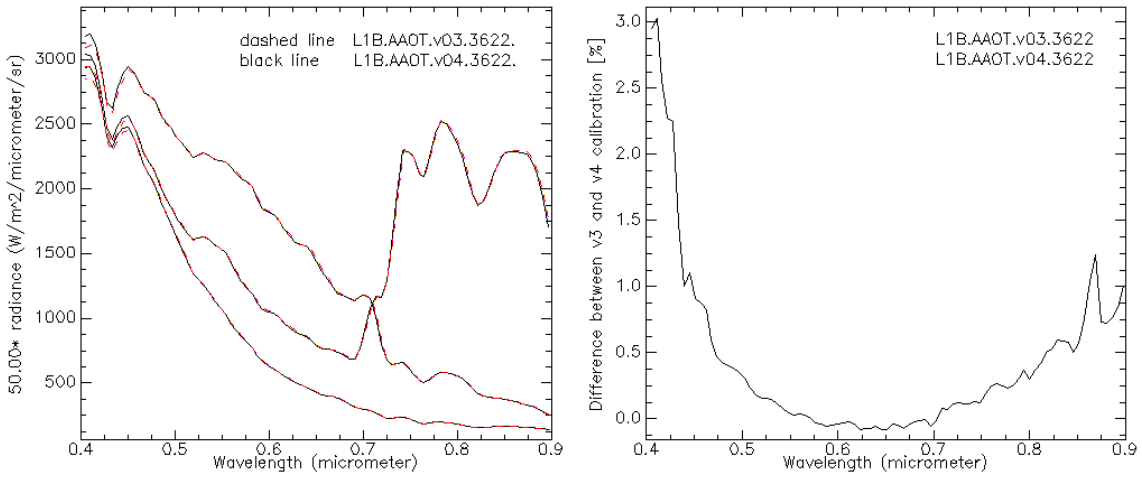

Figure 1 Comparison of calibrated radiance data version 03 and version 04. The compared HICO scenes are L1B.AAOT.v03.3622 and L1B.AAOT.v04.3622 from 8th August 2010 at AAOT in Venice.

Figure 1 shows a comparison of HICO calibrated radiance version 03 and 04 for HICO scenes L1B.AAOT.v03.3622[1] and L1B.AAOT.v04.3622[2] from 8th August 2010 at AAOT in Venice by plotting different spectral profiles in deep and shallow water as well as on land (left). The spectral profile average window was set to 11 x 11 pixels for each spectral profile. L1B radiance data of calibration version 04 was slightly higher in the blue and near infrared wavelength region. The graph on the right shows the average difference between calibration version 03 and version 04 in %. The observed differences were around 2.9 % at 445 nm and around 1 % at 860 nm. A wavelength shift of 0.9 nm was also found between the calibration versions 03 and 04. The same exercise was performed on the HICO scene L1BM.AAOT.v03.7339[3] and L1B.AAOT.v04.7339[4] from 22nd July 2011 at AAOT in Venice resulting in similar values.

[1] iss.2010220.0808.080016.L1B.AAOT.v03.3622

[2] iss.2010220.0808.080016.L1B.AAOT.v04.3622

[3] iss.2011203.0722.104757.L1BM.AAOT.v03.7399

[4] iss.2011203.0722.104757.L1BM.AAOT.v04.7399

4. Intercomparison of atmospheric correction methods

4.1 ATCOR and Tafkaa 6s comparison

The HICO scene L1B.AAOT.v03.3622 from 8th August 2010 at AAOT in Venice was used for this comparison. The Tafkaa model was only performed on the older calibration version 03, ATCOR was run on both calibration version (03 and 04). Only the results from calibration version 03 are shown for comparison (Figure 4).

Tafkaa 6s was run by Oregon State University (OSU) using a continental aerosol model and aerosol visibility of 60 km. ATCOR was run at DLR using similar settings (rural atmosphere and a visibility of 60 km).

4.1.1 Intercomparison EO Solar irradiance

The solar spectral irradiance used for the Tafkaa processing (Montes et al. 2004) was found to be consistently lower than the Fontenla et al. 2011 irradiance used for the ATCOR processing as shown in Figure 2. Thus, when the HICO radiance data are normalized to reflectance, this leads to lower reflectance values in ATCOR than in Tafkaa.

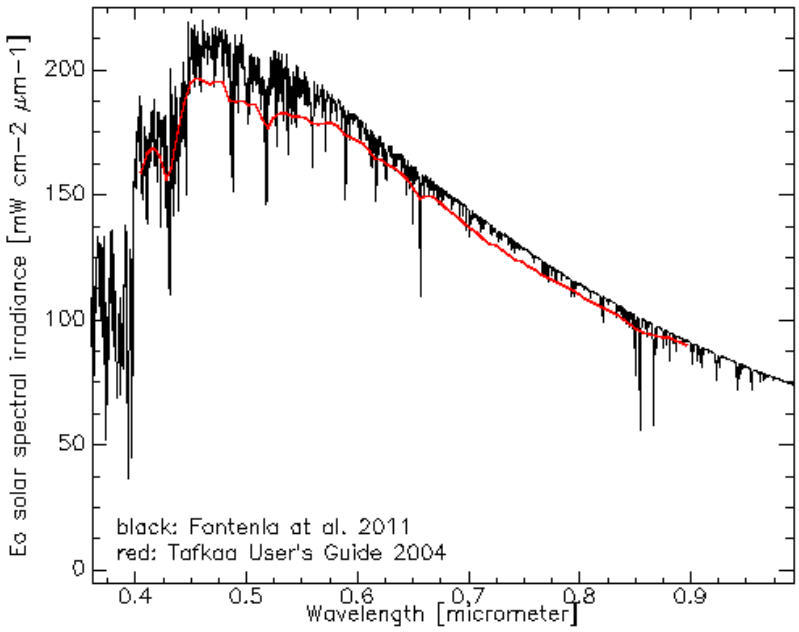

Figure 2 Comparison of EO solar spectral irradiance files. Black line is adapted from Fontenla et al. 2011 as used in ATCOR, the red line is the solar irradiance file as described by Montes et al. 2004 in the Tafkaa user's guide.

4.1.2 Aerosol optical thickness form AERONET-OC

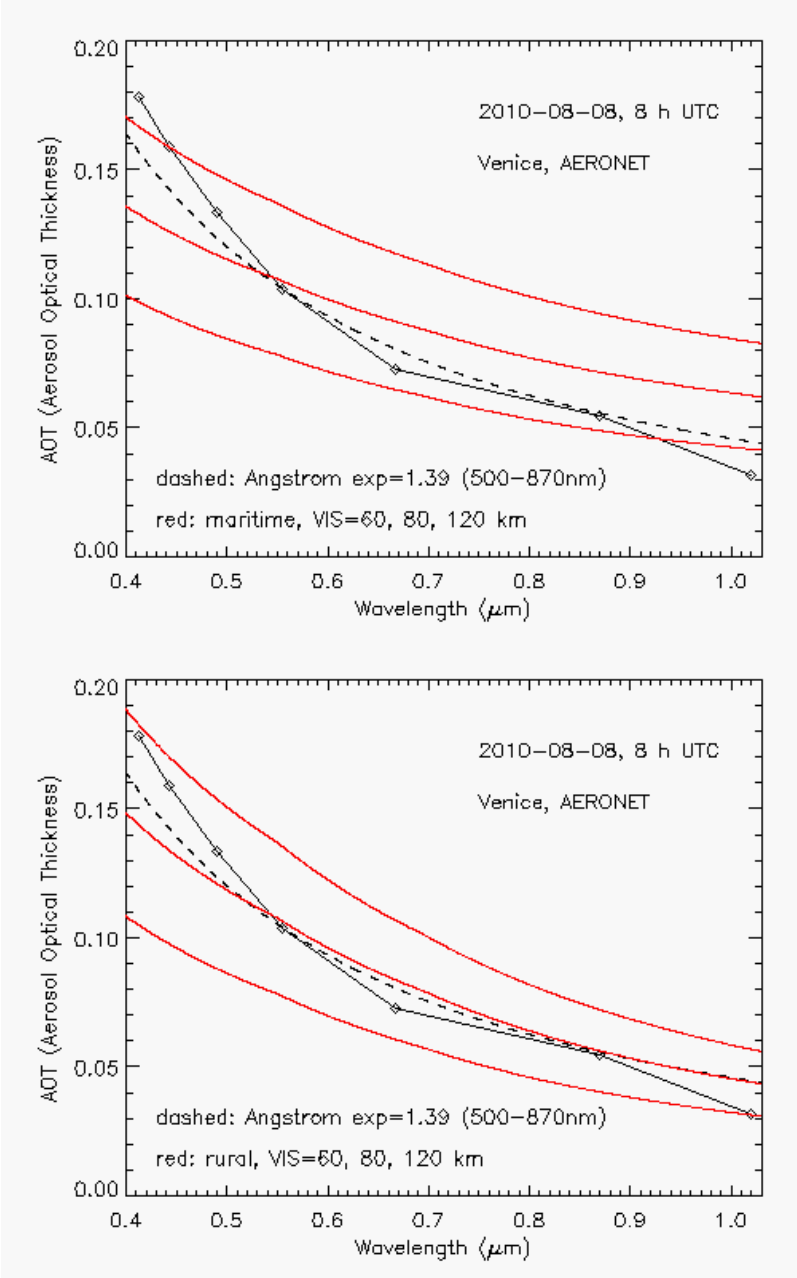

Figure 3 Specifying aerosol optical properties for ATCOR processing. Solid line marked with diamonds: AERONET measurements of AOT. For comparison: Aerosol optical thickness (AOT) of a maritime (top) and a rural (bottom) aerosol model calculated with 60, 80 and 120 km visibility using MODTRAN5.2 (red curves) and was compared to the Angstrom exponent (500-870 nm)(from AERONET)(Zibordi et al. 2009).

Figure 3 contains a comparison of the AERONET AOT (Zibordi et al. 2009) measurements (solid line with diamonds) and MODTRAN calculations for different visibilities and two aerosol types

(maritime and rural). It demonstrates that the rural aerosol with a visibility of 80 km approximates the spectral AOT course better than the maritime aerosol. A possible reason is that the wind at that time was blowing from the land to the coastal water area. The corresponding dashed curve presents the AOT behavior based on the AERONET Angstrom exponent using channels form 500 to 870 nm. The Angstrom approach yields a reasonable agreement with the measured curve, except for the blue spectral region.

4.1.3 Atmospherically corrected reflectance (ATCOR and Tafkaa 6s)

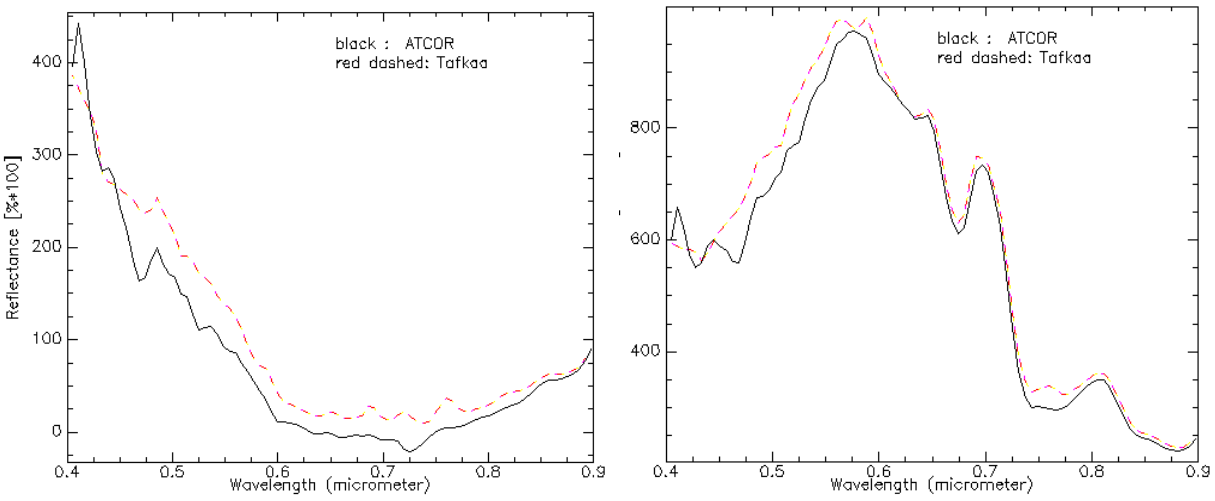

Figure 4a Comparison of ATCOR and Tafkaa 6s processing. The graphs show examples of reflectance spectra from two water pixels of atmospherically corrected HICO Scene L1B.AAOT.v03.3622 from 8th August 2010 at AAOT in Venice. Black lines shows ATCOR atmospheric correction model, red dashed lines shows results of Tafkaa 6s atmospheric correction model. The collected reflectance spectra are deep water spectra (left), and water spectra within the lagoon (right). The spectral profile average window was set to 11 x 11 pixels for each spectral profile.

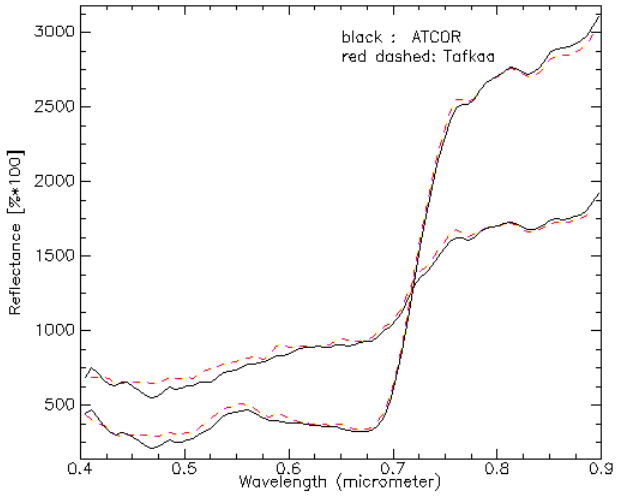

Figure 4b Comparison of ATCOR and Tafkaa 6s processing. The graphs show examples of reflectance spectra from two land pixels of atmospherically corrected HICO Scene L1B.AAOT.v03.3622 from 8th August 2010 at AAOT in Venice. Black lines shows ATCOR atmospheric correction model, red dashed lines shows results of Tafkaa 6s atmospheric correction model. The collected reflectance spectra are vegetated and urban land spectra from the same scene. The spectral profile average window was set to 11 x 11 pixels for each spectral profile.

Tafkaa 6s and ATCOR correspond well, although Tafkaa 6s shows continuously higher reflectance spectra than the ATCOR model. This effect is probably due to the lower Tafkaa solar irradiance spectrum (see Figure 2).

4.2 ATCOR and MIP comparison

The HICO scene L1BM.AAOT.v03.7339[5] from 22nd July 2011 at AAOT in Venice was used for this comparison.

The MIP processing was only performed on the older calibration version 03, ATCOR was also run on both calibration version (03 and 04). Only the results from calibration version 03 are shown for comparison (Figure 5).

[5] iss.2011203.0722.104757.L1BM.AAOT.v03.7399

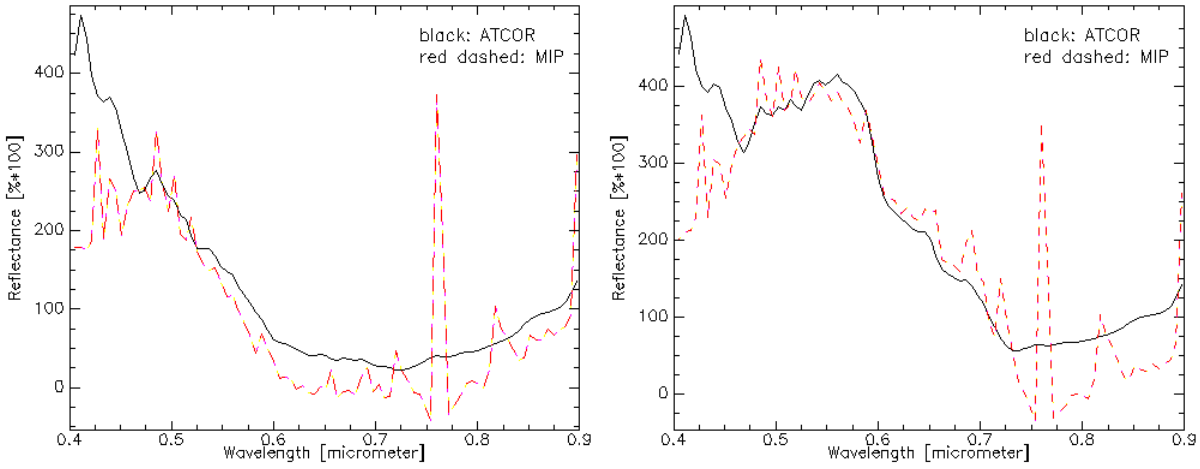

Figure 5 Comparison of MIP and ATCOR processing. HICO Scene L1BM.AAOT.v03.7339 from 22nd July 2011 at AAOT in Venice**.** The graph on the left shows a deep water spectrum and the graph on the right shows a water spectrum within the lagoon. The spectral profile average window was set to 11 x 11 pixels for each spectral profile.

The high peak at 760 nm in the MIP spectra (red dashed line) is due to oxygen absorption, whereas in ATCOR this peak was smoothed. The greatest difference is visible in the blue wavelength region, where the ATCOR reflectance is significantly higher than the MIP reflectance. This difference could be explained by the influence of different aerosol settings or due to calibration problems below 450 nm. Further processing is required to investigate this effect in more detail.

Both spectra show an increase in the NIR beyond 750 nm, which is also visible in the ATCOR-Tafkaa 6s comparison in Figure 4. The NIR reflectance behavior indicates that there is a processing or radiometric calibration problem in this region, because such an increase cannot be explained by water properties. The adjacency effect is probably not the cause since similar behavior is observed for all water pixels, irrespective of the distance to land. The consistent reflectance spectra from all three software indicate a radiometric calibration problem in the NIR region.

5. Water quality products using MIP

Fig. 6a and 6b shows first results of water quality products using MIP in-water processing algorithms. Both chlorophyll and suspended matter concentrations are higher near shore. A high correlation between them suggests that suspended matter is mainly of organic origin. Chlorophyll measurements at the Aqua Alta Oceanographic Tower in Venice (AAOT) (Lat 45.31°, Lon 12.50°) within 2 hours of the data take were 0.49 µg/l (from AERONET-OC).

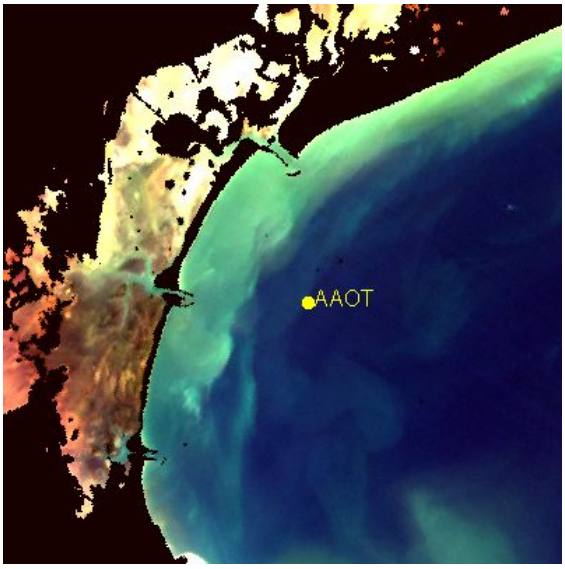

Figure 6a Water quality products using MIP. HICO Scene L1BM.AAOT.v03.7339 from 22nd July 2011 at AAOT in Venice. The scene was atmospherically and in-water processed using MIP software. The yellow dot shows the approximate location of the Aqua Alta Oceanograpic Tower (Lat 45.31°, Lon 12.50°) in Venice, located 18 km off the Venice Lagoon.

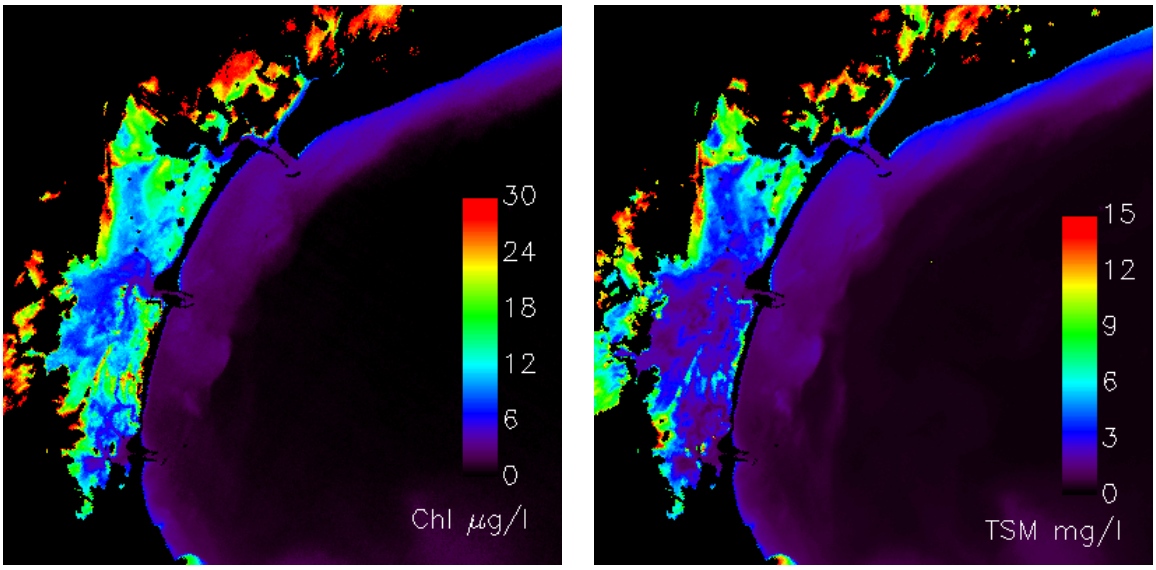

Figure 6b Water quality products using MIP. HICO Scene L1BM.AAOT.v03.7339 from 22nd July 2011 at AAOT in Venice. The scene was atmospherically and in-water processed using MIP software. It shows the distribution of chlorophyll in µg/l (left) and of suspended matter concentration in mg/l (right).

6. Conclusion

In this study two software comparisons were carried out using (1.) ATCOR and Tafkaa 6s and (2.) ATCOR and MIP. The two comparisons were done on different HICO scenes, so that a direct

comparison of all three processing methods was not possible. It is anticipated to do further processing on HICO data to provide more detailed analysis.

A first experiment shows that HICO measurements are promising for monitoring of water quality in the near-shore regions. The relatively high spatial resolution (for a water color instrument) and the large number of channels allow a detailed specification of water constituents.

HICO data generally deliver useful spectral information for land and water applications. However, there seems to be a radiometric calibration problem for channels beyond 750 nm, because the three atmospheric correction methods employed in this investigation (Tafkaa 6s, ATCOR, and MIP) consistently show a significant increase of clear water reflectance from 750 to 900 nm. This effect should be further investigated and probably requires another HICO data reprocessing.

7. References

Bachmann, M., Habermeyer, M., Holzwarth, S., Richter, R. , Müller, A. (2007): Including Quality Measures in an Automated Processing Chain for Airborne Hyperspectral Data, In: EARSeL Workshop on Imaging Spectroscopy, Bruges, Belgium .

Fontenla, J. M., J. Harder, W. Livingston, M. Snow, and T. Woods (2011): High-resolution solar spectral irradiance from extreme ultraviolet to far infrared, J. Geophys. Res., 116, D20108, doi:10.1029/2011JD016032.

Heege, T., Kisselev, V., Miksa, S., Pinnel, N., Häse, C. (2005): Mapping Aquatic Systems with a Physically Based Process Chain, In: SPIE Ocean Optics, Fremantle, Australia.

Montes, M.J., Gao, B.-C., Davis , C.O. (2004): NRL Atmospheric Correction Algorithms for Oceans: Tafkaa User's Guide, NRL/MR/7230--04-8760, Washington, DC .

Müller, R., Bachmann, M., Miguel, A., Müller, A., Neumann, A., Palubinskas, G., Richter, R. Schneider, M., Storch, T.,Walzel, T., Kaufmann, H., Guanter, L., Segl, K., Heege, T., Kiselev, V. (2010): The Processing Chain and Cal/Val Operations of the Future Hyperspectral Satellite Mission EnMAP, In: IEEE Aerospace Conferences. IEEE Aerospace Conference, Big Sky, Montana, USA.

Richter, R. (1996): A spatially adaptive fast atmospheric correction algorithm, International Journal of Remote Sensing, 17(6), 1201-1214.

Richter, R. (1998): Correction of satellite imagery over mountainous terrain, Applied Optics, 37(18), 4004-4015.

Richter, R., and Schläpfer, D. (2008): Considerations on water vapor and surface reflectance retreivals for a spaceborne imaging spectrometer, IEEE TGRS, 46(7), 1958-1966.

Richter, R., Schläpfer, D., Müller, A. (2011): Operational atmospheric correction for imaging spectrometers accounting for the smile effect, IEEE TGRS, 49(5), 1772-1780 .

Rossner, G., Schaadt, P., Chlebek, C., von Bargen, A. (2009): EnMAP – Germany's Hyperspectral Earth Observation Mission. Outline and Objectives of the EnMAP Mission, In: EARSeL SIG-IS Workshop, Tel Aviv, Israel.

Storch, T., de Miguel, A., Palubinskas, G., Müller, R., Richter, R., Müller, A., Guanter, L., Segl, K.,Kaufmann, H. (2009): Processing Chain for the Future Hyperspectral Mission, In: EARSeL SIG-IS Workshop, Tel Aviv, Israel.

Zibordi, G., Holben, B., Slutsker, I., Giles, D., D'Alimonte, D., Mélin, F., Berthon, J.-F., Vandermark, D., Feng, H., Schuster, G., Fabbri, B.E., Kaitala, S., Seppälä, J. (2009): AERONET-OC : A network for the validation of ocean color primary products, Journal of Atmospheric AND Oceanic Technology, Vol. 26, 1634 – 1651.

Acknowledgement

Our special thanks go to the whole HICO Team at NRL and OSU for providing the HICO data to us. In particular we wish to thank Curtiss O. Davis and Jasmine Nahorniak at Oregon State University, Corvallis OR for their outstanding support and service. Nicholas B. Tufillaro at Oregon State University parameterized the atmospheric correction for HICO using Tafkaa 6s as a special request. We also would like to thank Giuseppe Zibordi at JRC for providing access to the AERONET-OC data at AAOT.